AUGUST 28 2008

In situ measurements of velocity dispersion and attenuation in New Jersey Shelf sediments

Altan Turgut; Tokuo Yamamoto

J. Acoust. Soc. Am. 124, EL122–EL127 (2008)
https://doi.org/10.1121/1.2961404

In situ measurements of velocity dispersion and attenuation in New Jersey Shelf sediments

Altan Turgut
Naval Research Laboratory, Acoustics Division, Washington, DC 20375
turgut@nrl.navy.mil

Tokuo Yamamoto
University of Miami, RSMAS, Div. of Applied Marine Physics, Key Biscayne, Florida 33149
tyamamoto@rsmas.miami.edu

Abstract: The existence of acoustic velocity dispersion and frequency dependence of attenuation in marine sediments is investigated using *in situ* measurements from a wideband acoustic probe system during the Shallow Water 2006 experiment. Direct-path pulse propagation measurements show evidence of velocity dispersion within the 10–80 kHz frequency band at two silty-sand sites on the New Jersey Shelf. The measured attenuation in dB/m shows linear frequency dependency within the 10–80 kHz frequency band. The measured velocity dispersion and attenuation curves are in good agreement with those predicted by an extended Biot theory [Yamamoto and Turgut, J. Acoust. Soc. Am. **83**, 1744-1751 (1988)] for sediments with a distribution of pore sizes.

PACS numbers: 43.30.Ma, 43.20.Jr [WC]
Date Received: March 25, 2008 **Date Accepted:** June 19, 2008

1. Introduction

Compressional wave velocity and attenuation are two of the most important geoacoustic parameters that control sound propagation in shallow water. The existence of velocity dispersion and nonlinear frequency dependence of attenuation within the seabed might drastically change the predictions of propagation models that commonly use constant velocity and linear frequency dependence of attenuation. Several measurement techniques have been used to measure the compressional wave velocity and attenuation at different frequency bands in different types of marine sediments. Strong velocity dispersion in well-sorted beach sediments in the 1–30 kHz frequency band has been observed by using cross-probe measurements.[1] Critical-angle measurements of reflection coefficient[2] and shotgun/sediment-probe measurements[3] also indicated strong velocity dispersion in granular marine sediments. A lesser degree of velocity dispersion within the 25–100 kHz frequency region has been observed in medium-sand sediments in the Gulf of Mexico by using a sediment probe system.[4] More recent time-of-flight measurements by using buried source and receivers in the same area showed strong velocity dispersion within the 1–5 kHz region.[5] A reflection measurement technique[6] showed almost negligible velocity dispersion within the 0.1–10 kHz frequency region in silty-sand sediments of Malta Plateau and New Jersey Shelf. An earlier version of the wideband acoustic probe system[7] showed weak velocity dispersion in silty sediments and no velocity dispersion in muddy sediments within the 20–100 kHz frequency band. In this paper, wideband (10–80 kHz) measurements of velocity dispersion and attenuation in silty sand are reported.

In Sec. 2, a brief description of measurements and methods for measuring *in situ* velocity dispersion and attenuation are given. Then, measured velocity dispersion and attenuation are compared with those calculated from an extended Biot model.[8] In Sec. 3, the extended Biot model is briefly described and sound speed and attenuation predictions are presented for sediments having different distribution of pore sizes. Finally, in Sec. 4, summary and conclusions are given.

2. Experiment

As a part of sediment charcterization effort during the SW06 experiment, a wideband acoustic probe system was deployed at two different sites on the New Jersey Shelf. At Site-1 (39.0235N, 73.0348W), additional high-frequency scattering and propagation measurements were conducted. At Site-2 (39.00145N, 73.1202W), independent measurements of sound speed, density, porosity, and grain size were available from a 3-m-long sediment core. The acoustic probe system includes a self-contained data acquisition unit, four acoustic probes (one source and three receivers), and about 400 kg of lead weights. The self-contained data acquisition unit is programmed on board the research vessel based on a planned pulse transmission schedule. The system can be operated at water depths up to 2000 m with up to 2 m penetration into the sediment. Each probe is 20 mm in diameter and has an adjustable length. The acoustic transducers are cylindrical rings with OD=15 mm, ID=12 mm, and height=20 mm. Loading effects might be significantly different when the acoustic transducer is placed in hard (sandy) sediments than those in the water column. These differences might introduce measurement errors if the waveforms measured by a single receiver in the water and sediment. In our measurements, the wideband pulse signals received at two buried receivers are used for measuring velocity and attenuation as a function of frequency. Spectral ratio method[1] is used to calculate and phase velocity and attenuation from the measured pulse spectra. The phase delay between two receivers is calculated as

$$\Delta\phi(\omega) = \tan^{-1}\{\mathrm{Im}[S_2(\omega)/S_1(\omega)]/\mathrm{Re}[S_2(\omega)/S_1(\omega)]\}, \tag{1}$$

where $S_1(\omega)$ and $S_2(\omega)$ are spectra of the pulses received at distances d_1 and d_2, respectively. When the distance between two receivers is larger then the acoustic wavelengths, the above equation provides a wrapped phase delay in the range $[-\pi\ \pi]$. To remove the phase wrapping, a reference velocity c_0 is used to align the received pings by applying a constant phase shift to $S_2(\omega)$ as $S_2'(\omega)=S_2(\omega)\exp[-i\omega(d_2-d_1)/c_0]$. In Eq. (5), the spectrum $S_2(\omega)$ is replaced by $S_2'(\omega)$ and a new phase delay $\Delta\phi'$ is obtained. Then, the phase speed is calculated using the new phase delay as

$$c_p = c_0\left(1+\frac{c_0\Delta\phi'}{\omega(d_2-d_1)}\right)^{-1}. \tag{2}$$

The spectral ratio of two pulses received by two receivers is also used for measuring attenuation as a function of frequency. Spectral ratios are calculated both in the water column and sediment so that geometrical spreading and different receiver sensitivities can be taken into account automatically. The attenuation in dB/m is calculated from the spectral ratio as

$$\alpha = \frac{8.686}{(d_2-d_1)}\ln[|S_1(\omega)/S_2(\omega)|/|Q_1(\omega)/Q_2(\omega)|], \tag{3}$$

where $Q_1(\omega)$ and $Q_2(\omega)$ are spectra of the pulses transmitted in water and received at distances d_1 and d_2, respectively. Three Gaussian-windowed LFM pulses (5–25 kHz, 20–50 kHz, and 40–100 kHz) are transmitted by the source transducer, and measured pulse spectra $S_1(\omega)$ and $S_2(\omega)$ are used in Eqs. (1)–(3) to calculate phase velocity and attenuation. Figure 1 shows the measured phase velocity and attenuation at Site-1 and Site-2. Note that compressional wave velocity gradually increases for each frequency band from 10 to 80 kHz. The velocity dispersion is slightly stronger at the Site-1 especially within 30–40 kHz frequency band. The gaps in the measured data are due to the discarded low signal to noise ratio regions at both sides of the Gaussian-shaped spectra. An extended Biot theory, described in the next section, was used to calculate velocity and attenuation curves for silty sand with a log-normal pore-size distribution. The sediment physical properties, used in the calculations, are inferred from the core data and given in Table 1. The calculated phase velocity and attenuation curves are also plotted in Fig. 1 with pore-size standard deviations of $\sigma=0.0$, $\sigma=1.25$, and $\sigma=2.0$. The Biot theory with the

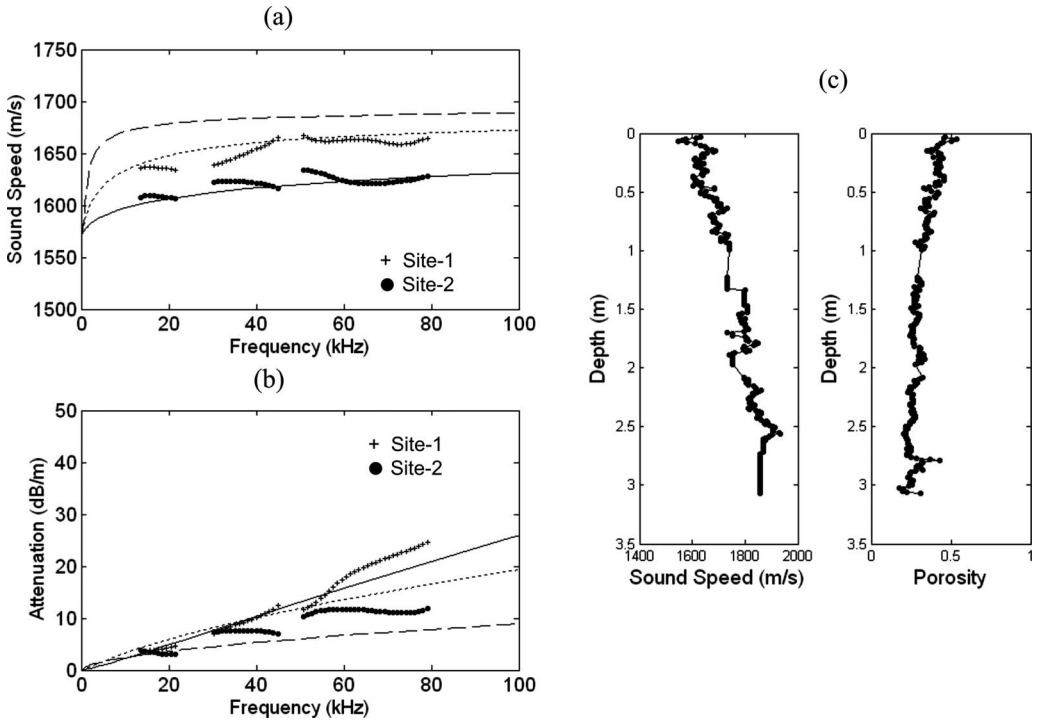

Fig. 1. (a-b) Comparison of measured velocity and attenuation curves with those calculated by using the extended Biot theory. The physical properties in Table I with pore-size standard deviations of $\sigma=0.0$ (long-dashed line), $\sigma=1.25$ (dashed line), and $\sigma=2.0$ (solid line) are used in the calculations. (c) Velocity and porosity profiles obtained from a sediment core near Site-2.

uniform pore size assumption ($\sigma=0.0$) predicts a dispersion region below 10 kHz and there is no significant dispersion within the 10–80 kHz frequency band. The extended Biot theory predictions agree with the measurement results when silty-sand sediments, with pore-size standard deviations between $\sigma=1.25$ and $\sigma=2.0$, are considered. In Fig. 1(b), measured and calculated attenuation coefficients are compared. The measured attenuation values are in agreement with the theoretical predictions when sediments with distributed pore sizes are considered. Figure

Table 1. Physical properties and their values used in the calculation of sound speed and attenuation.

Physical Property	Symbol	Unit	Value
Grain density	ρ_r	kg/m^3	2650
Fluid density	ρ_f	kg/m^3	1024
Grain bulk modulus	K_r	N/m^2	3.6×10^{10}
Frame bulk modulus	K_s	N/m^2	3.69×10^{7}
Fluid bulk modulus	K_f	N/m^2	2.33×10^{9}
Shear modulus	μ	N/m^2	2.61×10^{7}
Dynamic viscosity of pore fluid	η	kg/m/s	1.0×10^{-3}
Permeability	k_s	m^2	5.0×10^{-11}
Porosity	β	⋯	0.46
Shear specific loss	δ_s	⋯	0.1
Frame volumetric specific loss	δ	⋯	0.05
Added mass coefficient	α	⋯	0.25

1(c) shows velocity and porosity profiles near Site-2, obtained from the sediment core analysis. At the probe depths (0.5 m), the sound velocities measured by a 500 kHz acoustic core logger are slightly higher than those measured by the *in situ* acoustic probe system. Grain size analysis at the probe depth (0.5 m) showed a mixture of gravel (11%), sand (70%), silt (12%), and clay (7%) at Site-2. Assuming a correlation between grain size and pore size distributions, this confirms our acoustic prediction of nonuniform ($\sigma \neq 0$) pore size distribution. The frequency dependency of the attenuation in sediments with various pore-size distributions will be elaborated in the next section.

3. Extended Biot theory predictions

Marine sediments can be regarded as a fluid-filled porous medium, and acoustic wave interaction with the bottom can be physically modeled by Biot's theory.[9] An extension of the Biot theory has been developed[8] for marine sediments with statistically distributed pore sizes and successfully validated for air-filled porous granular materials.[10] In the Biot theory, acoustic wave attenuation is primarily attributed to the viscous losses due to relative motion between the pore fluid and the skeletal frame. The viscous interaction is assumed to take place according to Darcy's law of fluid flow through porous media with the modification that the viscosity is made dependent on the frequency of the elastic wave. A frequency dependent viscosity correction factor, F, is defined by comparing the ratio of the total friction to the average fluid velocity in the oscillatory flow and steady laminar flow regimes. It is also assumed that the variation of viscous friction with frequency in a porous material follows the same laws as that in a single pore represented by a two-dimensional duct or a capillary tube of uniform cross section. Yamamoto and Turgut[8] have suggested a new viscous correction factor by calculating total viscous resistance and average seepage velocity for a macroscopic unit element with nonuniform pore size distribution. The new viscous correction factor is calculated as

$$F(\omega) = \frac{k_s}{\beta} \frac{2\int_0^\infty r^{-2}\kappa K(\kappa)e(r)dr}{\int_0^\infty [1 + 2iK(\kappa)/\kappa]e(r)dr}, \tag{4}$$

where $\kappa = r(\omega\rho_f/\eta)^{1/2}$ is a nondimensional parameter, ω is the angular frequency, k_s is the permeability, β is the porosity, r is the pore radius, $e(r)$ is the pore radius distribution function, η is the dynamic viscosity, ρ_f is the pore fluid density, and

$$K(x) = \frac{\mathrm{ber}'x + \mathrm{bei}'x}{\mathrm{ber}x + \mathrm{bei}\,x}, \tag{5}$$

in which ber and bei are the real and imaginary parts of Kelvin function and ber' and bei' are their derivatives.

In Fig. 2, pore size distributions of New Jersey Shelf sediments, measured by mercury injection technique, are shown. The pore-size distributions in Figs. 2(a) and 2(b) are approximated as log-normal [or ϕ-normal, $\phi = -\log_2 r$ (r in mm))] radius distributions with the standard deviation σ and mean $\bar{\phi}$ [$\sigma = 1.5$, $\bar{\phi} = 5.5$ in Fig. 2(a), and $\sigma = 2.2$, $\bar{\phi} = 7.8$ in Fig. 2(b)]. In Fig. 3, the measured and calculated phase velocity and attenuation curves are plotted in logarithmic scale to identify the velocity dispersion regions and to examine the frequency dependency of attenuation. In Figs. 3(a) and 3(b), it can be seen that, in sediments with nonuniform pore size distribution, the velocity dispersion and nonlinear attenuation regions due to viscous friction, are widened and shifted toward higher frequencies. Again, theoretical predictions by using $\sigma = 1.25$, and $\sigma = 2.0$ agree with the measured velocity and attenuation much better than that of using $\sigma = 0.0$. In Figs. 3(c) and 3(b), theoretical predictions of frequency dependency of attenuation are shown for $\sigma = 0.0$, $\sigma = 1.25$, and $\sigma = 2.0$. Using the definition $\alpha = kf^n$ (k is a constant and f is the frequency in kHz), the power exponents of $n = 0.6$, $n = 0.79$, and $n = 1.0$ are found by line fitting within the 10–100 kHz band. Similarly, within the 0.1–1 kHz frequency band, power exponent values of $n = 1.74$, $n = 1.45$, and $n = 1.35$ are found for $\sigma = 0.0$, $\sigma = 1.25$, and $\sigma = 2.0$, respectively. Sediments with sand, silt, and clay mixture are represented by higher values of σ,

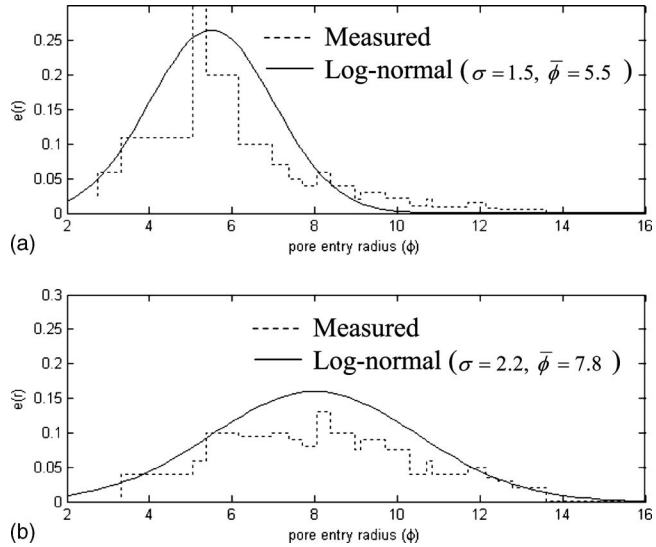

Fig. 2. Pore size distribution of New Jersey sediments measured by Mercury Injection technique (dashed lines). The log-normal pore-size distribution model with (a) σ=1.5, $\bar{\phi}$=5.5, and (b) σ=2.2, $\bar{\phi}$=7.8, are also shown (solid lines).

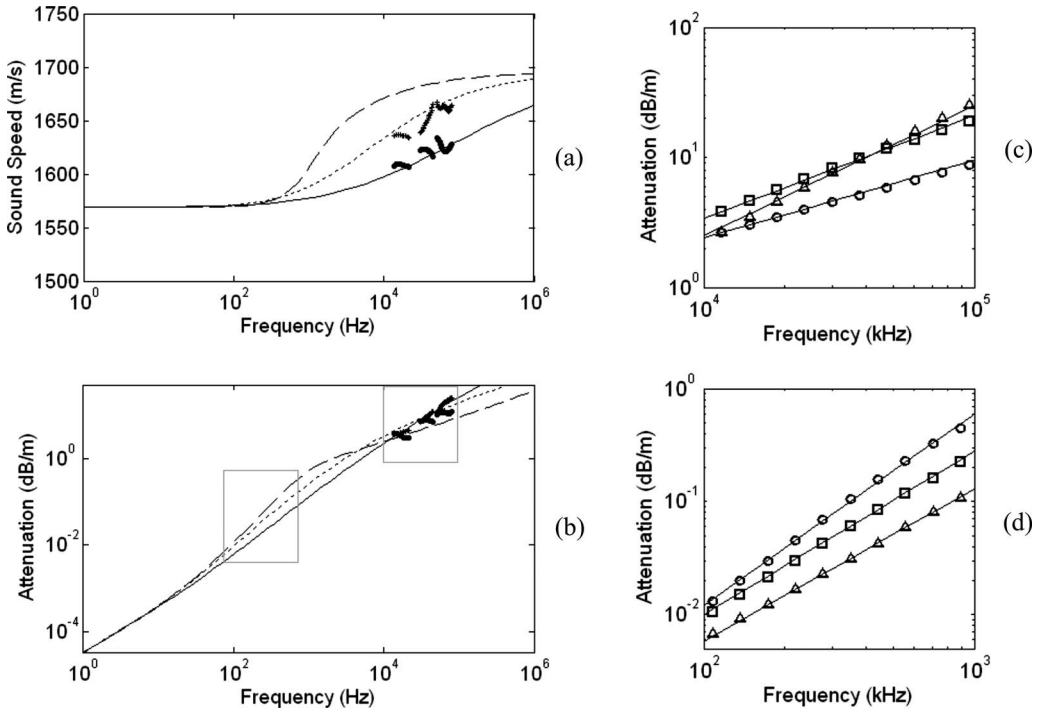

Fig. 3. (a-b) Comparison of measured velocity and attenuation curves with those calculated by using the extended Biot theory plotted in logarithmic scales [σ=0.0 (long-dashed line], σ=1.25 (dashed line), and σ=2.0 (solid line), (c-d) frequency dependency of attenuation at high- and low-frequency band, for σ=0.0 (circle), σ=1.25 (square), and σ=2.0 (triangle).

while sediments with more uniform grain sizes are represented by smaller value of σ, indicating more uniform pore sizes. Within the 0.1–1 kHz frequency band, the estimated power exponents are in good agreement with that of several low-frequency measurements, recently reported by Holmes *et al.*[11]

4. Summary and conclusions

In situ measurements of sound speed and attenuation were performed by using a wideband acoustic probe system, deployed at two silty-sand sites on the New Jersey Shelf. The spectral ratios of broadband pulses, transmitted between the 0.5-m-deep probes, showed phase velocity dispersion within the 10–80 kHz frequency band. The frequency region of observed velocity dispersion seems to be higher than that of previous measurements, performed in well-sorted beach sand and granular marine sediments.[1,3,5] As compared to the original Biot theory predictions, measured phase velocity dispersion results agree better with those predicted by the extended Biot theory with nonuniform pore size distribution. The observed linear frequency dependency of the attenuation also agrees with the theoretical predictions when sediments with nonuniform pore size distributions are considered.

Acknowledgments

This work was supported by the Office of the Naval Research. The authors thank the crew of the R/V Knorr for the excellent support during the 2006 Shallow Water Experiment. They also thank Chief Scientist Dr. D. J. Tang for the scientific support.

References and links

[1]A. Turgut and T. Yamamoto, "Measurements of acoustic wave velocities and attenuation in marine sediments," J. Acoust. Soc. Am. **87**, 2376–2382 (1990).
[2]A. Maguer, E. Bovio, and W. L. J. Fox, "Mechanisms for subcritical penetration into a sandy bottom: Experimental and modeling results," J. Acoust. Soc. Am. **107**, 1215–1225 (2000).
[3]R. D. Stoll, "Velocity dispersion in water-saturated granular sediment," J. Acoust. Soc. Am. **111**, 785–792 (2002).
[4]M. Buckingham and M. Richardson, "On tone-burst measurements of sound speed and attenuation in sandy marine sediments," IEEE J. Ocean. Eng. **27**, 413–428 (2002).
[5]J. C. Osler, A. P. Lyons, P. C. Hines, J. Scrutton, E. Pouliquen, D. Jones, D. M. F. Chapman, M. O'Connor, D. Caldwell, M. MacKenzie, I. B. Haya, and D. Nesbitt, "Measuring sound speed dispersion at mid to low frequency in sandy sediments: An overview of complementary experimental techniques developed for SAX04," In Underwater Acoustic Measurements: Technologies & Results, Heraklion, Crete, edited by John S. Papadakis and Leif Bjorno, 28th June—1st July (2005).
[6]C. W. Holland, J. Dettmer, and S. D. Dosso, "A technique for measuring in-situ compressional wave velocity dispersion in marine sediments," IEEE J. Ocean. Eng. **30**(4), 748–763 (2005).
[7]A. Turgut, R. Gauss, and J. Osler, "Measurements of velocity dispersion in marine sediments during the Baundary04 Malta plateau experiment," *Proceedings of the OCEANS 2005 MTS/IEEE, ISBN CD-ROM:* 0-933957-33-5 (2005).
[8]T. Yamamoto and A. Turgut, "Acoustic wave propagation through porous media with arbitrary pore size distributions," J. Acoust. Soc. Am. **83**, 1744–1751 (1988).
[9]M. A. Biot, "Theory of propagation of elastic waves in fluid-saturated porous solid: II High frequency range," J. Acoust. Soc. Am. **28**, 168–178 (1956).
[10]K. V. Horoshenkov and M. J. Swift, "The acoustic properties of granular materials with pore size distribution close to log-normal," J. Acoust. Soc. Am. **100**(5), 2371–2378 (2001).
[11]J. D. Holmes, W. M. Carey, S. M. Dediu, and W. L. Siegmann, "Nonlinear frequency dependent attenuation in sandy sediments," J. Acoust. Soc. Am. **121**(5), EL218–222 (2007).